Bis(imino)carbazolate a master key for barium chemistry

Peter Chapple, Samia Kahlal, Julien Cartron, Thierry Roisnel, Vincent Dorcet, Marie Cordier, Jean-Yves Saillard, Jean-François Carpentier, Yann Sarazin

Bis(imino)carbazolate: a master key for barium chemistry

Peter M. Chapple, Samia Kahlal, Julien Cartron, Thierry Roisnel, Vincent Dorcet, Marie Cordier, Jean-Yves Saillard,* Jean-François Carpentier and Yann Sarazin*

Dedicated to Professor Cristian Silvestru on the occasion of his 65th birthday.

P. M. Chapple, Dr. S. Kahlal, J. Cartron, Prof. Dr. J.-Y. Saillard, Dr. T. Roisnel, Dr. V. Dorcet, M. Cordier, Prof. Dr. J.-F. Carpentier, Dr. Y. Sarazin
Univ Rennes, CNRS, ISCR-UMR 6226, 35000 Rennes (France)
E-mail: yann.sarazin@univ-rennes1.fr
jean-yves.saillard@unic-rennes1.fr

Supporting information for this article is given via a link at the end of the document.

Abstract: We report here on a readily available bis(imino)carbazole-based proligand that constitutes a most convenient entry point into the challenging synthetic molecular chemistry of barium. It enables the preparation of rare or even, up to now, unknown, solution stable heteroleptic barium complexes. The syntheses and structural features for the first molecular Ba-fluoride and for the first Ba-stannylide with an unsupported Ba-to-Sn bond are described, along with other carbazolate barium species: an amide (both a remarkably stable starting material and an excellent hydrophosphination precatalyst), iodide, and silanylide. DFT analysis of bonding patterns in the Ba-stannylide and Ba-silanylide highlights a prevailingly ionic Ba-to-tetrelide bond with a small covalent contribution.

Introduction

Although the organometallic chemistry of the heavier group 2 alkaline earths (Ae = Ca, Sr, Ba) has received considerable attention in the past two decades,[1-6] it still lags behind the chemistry of the transition metals and that of the lanthanides. This is primarily due to the extreme oxophillic nature of the Ae metals, their strong ionic character and hence their tendency to redistribute ligands in solution through the Schlenk equilibrium. These issues are generally overcome by using bulky chelating ancillary ligands to inhibit Schlenk redistribution to homoleptic species that are either unreactive or uncontrollably reactive, or to insoluble polynuclear species. However, with the exception of a few examples, the limited range of appropriate ligands have hampered the use of these metals in organometallic processes, especially for the largest and most electropositive barium. Despite the problems associated with Ae metals, many examples exist in the recent literature of catalytic processes using low Ae catalyst loadings and mild conditions,[1-4] e.g. olefin hydroelementation,[7-9] imine[10] or alkene[11] hydrogenation, and dehydrocoupling of amines with hydrosilanes[12] or boranes.[13] For the chemistry of the heavier Ae metals, no ligand is more ubiquitous than 2,6-bis-diisopropylphenyl-β-diketiminate (BDI^{DiPP}, Fig. 1). Although well suited for calcium and to a lesser extent strontium complexes, for barium this ligand quickly redistributes to the unreactive homoleptic $[Ba\{BDI^{DiPP}\}_2]$.[14] Several sterically congesting monoanionic ligands have been reported that partially address this problem, including *N*-based systems such as the β-diketiminate derivative $\{BDI^{DiPeP}\}^-$,[15] a dipyrromethene,[16] a hydrotris(pyrazolyl)borate[17] or an iminoanilide,[18] and also cyclopentadienyl derivatives.[19] However, due to either synthetic difficulty or insufficient stabilising properties, none of these ligands have yet been widely adopted.

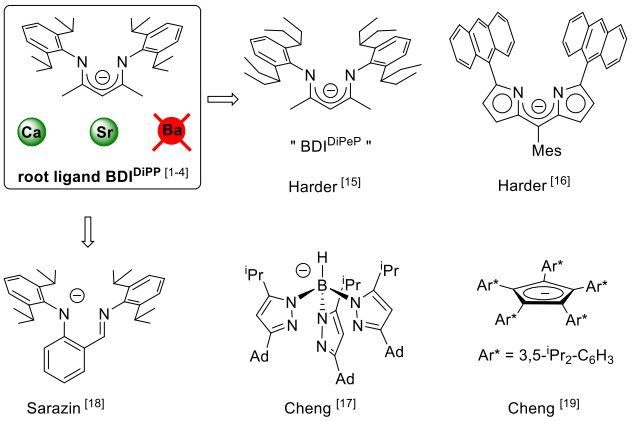

Figure 1. Examples of ligands used to stabilise heteroleptic Ba-complexes. (Mes = mesityl, Ad = 1-adamantyl). *NB*: BDI^{DiPP} is *not* suitable for barium.[14]

A variety of long sought *heteroleptic* calcium complexes have recently been prepared by utilising the BDI^{DiPP} ligand. Soluble Ca-hydroxide,[20] cyanide,[21] fluoride,[22] and triphenylstannylide[23] are hence now available. Related BDI^{DiPP}-strontium hydroxides and halides (including fluoride) have also been disclosed.[24-25] Yet, the corresponding chemistry of barium is still to be initiated, as it has been plagued by the absence of stable precursors. A handful of *homoleptic* Ca-tetrelides related to Hill's $[\{BDI^{DiPP}\}CaSnPh_3]_2$ also exist, e.g. $[Ca(TetR_3)_2(donor)_x]$ (Tet = Si, Ge, Sn), but congeneric strontium and barium species are still rare and known only for Si or Ge.[23,26-32] Ba-to-Sn bonds remain elusive, although ion pairs such as $[Ba(18\text{-c-}6).(HMPA)_2][SnPh_3]_2$ are known.[27]

Reported here is a tailor-made bis(imino)carbazolate capable of kinetically stabilising a range of highly reactive complexes of the heavier alkaline earths, including the first heteroleptic barium silanylide and stannylide complexes, along with the first molecular Ba-fluoride that completes the series of heavier Ae fluorides. The nature of the Ba-to-Sn and Ba-to-Si bonding is discussed in the light of DFT computations.

Results and Discussion

The bulky proligand 1,8-bis-(2,6-diisopropylphenyl)imino-3,6-di-*tert*-butyl-carbazole (aka {Carb^{DiPP}}H) is synthesised in ca. 70% yield and scales up to 25 g from the condensation between 2,6-diisopropylaniline and the reported 1,8-diformyl-3,6-di-*tert*-butyl-carbazole (Scheme 1).[33] The carbazole core and the two C=N moieties are coplanar. The N_{imine}-N(H)-N'_{imine} angle (97.31(8)°, SI Fig. S23) is well below that in 2,5-bis-{(2,6-diisopropylphenyl)-imino}pyrrole (133.16(5)°) used to obtain Ae-iodides.[34] We anticipated that {Carb^{DiPP}}$^-$ would provide a more sterically sheltered coordination sphere around the large Ba^{2+} cation (r_{ionic} = 1.35 Å) and afford stable complexes. The ligand was hence used to synthesise yet unknown barium species through protonolysis, transmetallation sequences (Scheme 1).

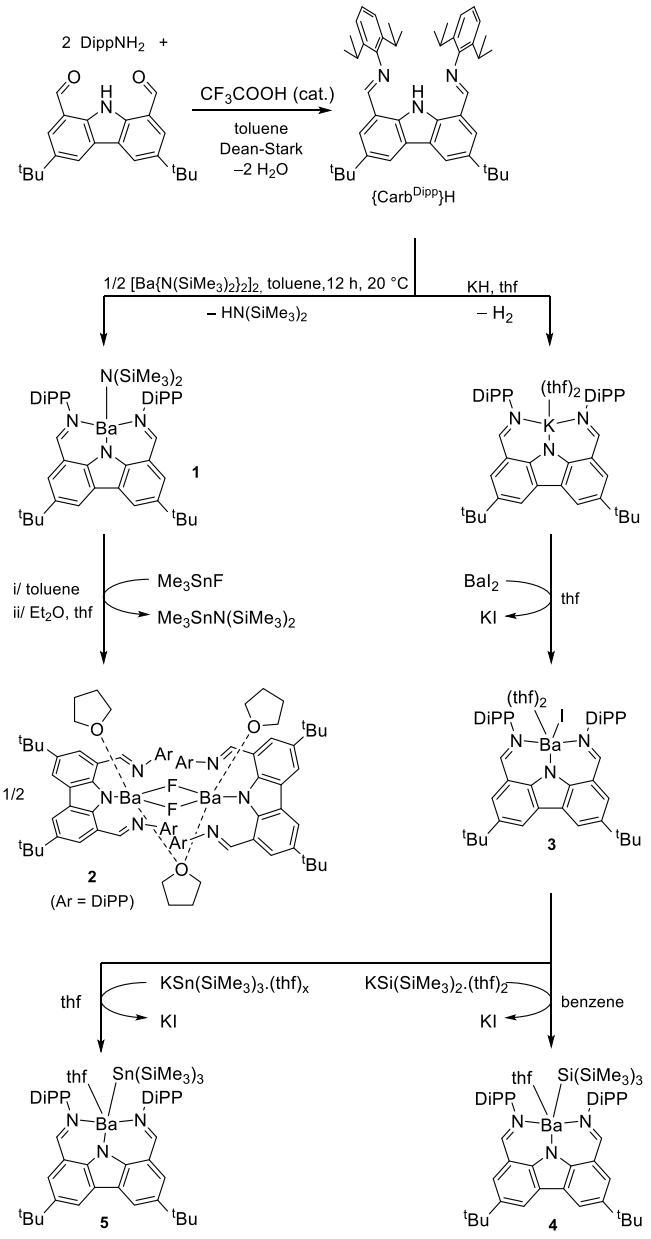

Scheme 1. Synthesis of bis(imino)carbazolate-barium amide (**1**), halides (**2**-**3**) and tetrelides (**4**-**5**), using the proligand {Carb^{DiPP}}H, where DiPP = 2,6-^{i}Pr$_2$-C$_6$H$_3$.

The unsolvated Ba-amide [{Carb^{DiPP}}BaN(SiMe$_3$)$_2$] (**1**) is conveniently obtained as a yellow solid upon stoichiometric reaction of {Carb^{DiPP}}H with [Ba{N(SiMe$_3$)$_2$}$_2$]$_2$. It is stable in solution in [D$_6$]benzene, without signs of decomposition or ligand redistribution after 20 days at 60 °C (Fig. S24). Complex **1** forms a four-coordinate monomer in the solid state, with a distorted tetrahedral environment (Fig. 2). The various Ba-N interatomic distances are commensurate with those in the iminoanilide [{N^N^{DiPP}}BaN(SiMe$_3$)$_2$.(thf)$_2$],[18] arguably the closest relative to **1**; the Ba-N_{imine} and Ba-$N_{carbazolate}$ interatomic distances are very similar (2.722(3)-2.741(3) Å).

The resilience of **1** to ligand scrambling contrasts with the known instability of [{BDI^{DiPP}}BaN(SiMe$_3$)$_2$.(thf)$_2$].[14] Gratifyingly, the deliberate formation of the otherwise undesired homoleptic [{Carb^{DiPP}}$_2$Ba] is only achieved under forcing conditions (80 °C, 16 h), with a three-fold excess of {Carb^{DiPP}}H vs [Ba{N(SiMe$_3$)$_2$}$_2$]$_2$. Yet, the reaction is not clean nor quantitative, as the product is still contaminated by the presence of **1**. It is likely that the congested environment around the metal precludes the easy coordination of a second bulky carbazolate.

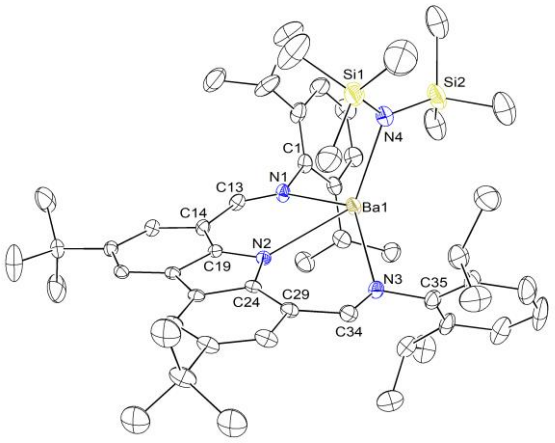

Figure 2. Displacement ellipsoids (30% probability; H atoms omitted) for [{Carb^{DiPP}}BaN(SiMe$_3$)$_2$] (**1**). Only one of the two independent but similar molecules in the asymmetric cell, and the main component of disordered ^{t}Bu and SiMe$_3$ groups, are depicted. Representative interatomic distances (Å) and angles (°): Ba1-N1 = 2.741(3), Ba1-N2 = 2.722(3), Ba1-N3 = 2.739(3), Ba1-N4 = 2.585(4); N1-Ba1-N3 = 133.13(10), N2-Ba1-N4 = 125.61(11).

Note also that THF-free **1** is prepared by a simple protonolysis protocol carried out overnight at 20 °C, or within 1 h at 60 °C, easier to implement than that for [{BDI^{DiPP}}AeN(SiMe$_3$)$_2$.(thf)$_x$]. These complexes, only stable in solution for Ae = Ca, are prepared by salt metathesis between AeI$_2$, {BDI^{DiPP}}H and KN(SiMe$_3$)$_2$ (2 eq.), and can only be isolated as thf solvates following this route.[14] Harder's bulkier {BDI^{DiPeP}}H does generate solvent-free [{BDI^{DiPeP}}AeN(SiMe$_3$)$_2$] stable for Ca-Ba, but requires heating at 140 °C for 5-9 days.[15]

The stability and availability of **1**, combined to the absence of coordinated solvent, make it an excellent precursor not only for synthetic but also for catalysis purposes. For instance, in the benchmark catalysis of the hydrophosphination of styrene with HPPh$_2$ (1:1 ratio, 3 mol-% **1**) that yields regioselectively PhCH$_2$CH$_2$PPh$_2$, **1** comes second to none. Its turnover frequencies, as high as 23 h^{-1} at 25 °C, betters those of the best

precatalysts known to date which, additionally, require higher temperatures to be effective (60-75 °C, Table S25).[4,35-36]

Besides, **1** reacts with Me_3SnF to return the dinuclear [({Carb^{DiPP}}Ba(μ-F).thf)$_2$(μ-thf)] (**2**) as a yellow crystalline solid. Complex **2** is the first molecular barium-fluoride, and completes the series of available heavier Ae-F species, over 10 years after the first soluble, molecular calcium-fluorides were unveiled.[22,25,37] It can be seen as a well-defined derivative of BaF_2 used for applications as sensors or windows in spectrometry due to its transparency from UV to far-IR. The C_2-symmetric dinuclear **2** is bridged by two F atoms and a thf molecule (Fig. 3). In addition to a carbazolate ligand, coordinative saturation around each metal is achieved by a thf molecule, making them seven-coordinated. The Ba-N_{imine} interatomic distances in **2** (2.937(3)-2.955(3) Å) are much longer than in **1**, reflecting greater coordination number and steric congestion about the metals in the fluoro complex. On the other hand, the Ba-$N_{carbazolate}$ distances in the two complexes are similar. For comparison, the coordination pattern in **2** differs from those in Ca/Sr fluorides. [{BDI^{DiPP}}Ca(μ-F).(thf)]$_2$ is a symmetrical dimer with one metal-bound thf molecule per Ca atom (Ca-F = (2.180(2)$_{av}$ Å).[22] Its strontium analogue, [{BDI^{DiPP}}Sr(thf)(μ-F)$_2$Sr{BDI^{DiPP}}(thf)$_2$], is asymmetrically ligated: one Sr atom bears one coordinated thf molecule, and the other carries two of them (Sr-F = 2.348(1)$_{av}$ Å).[25] The ^{19}F NMR spectrum of **2** recorded in [D_6]benzene at 23 °C features a single resonance, a somewhat broad singlet at δ_{19F} = +10.1 ppm. It is considerably deshielded compared to those in the abovementioned strontium (–60.0 ppm in [D_8]thf) and calcium (–78.0 ppm in [D_6]benzene) fluorides. The ^{19}F chemical shift in Ae-fluorides hence increases with metal electropositivity and polarity of the Ae-to-F bond, but this trend perhaps ought to be considered with caution as both coordination environments and NMR solvents vary for the three complexes.

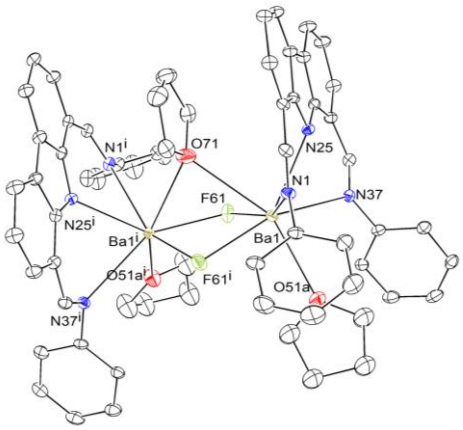

Figure 3. Displacement ellipsoids (30% probability; H atoms omitted) for [({Carb^{DiPP}}Ba(μ-F).thf)$_2$(μ-thf)] (**2**). Only the main components of disordered thf molecules and ^{t}Bu and ^{i}Pr groups depicted. ^{t}Bu and ^{i}Pr groups omitted for clarity. Representative interatomic distances (Å) and angles (°): Ba1-F61 = 2.511(2), Ba1-F61^i = 2.518(2), Ba1-N1 = 2.955(3), Ba1-N25 = 2.735(3), Ba1-N37 = 2.937(3), Ba1-O51A = 2.795(3), Ba1-O71 = 3.047(3); N1-Ba1-N37 = 112.92(8). Symmetry transformation: –x+1/2, y, –z+1/2.

The orange alkali salt [{Carb^{DiPP}}K.(thf)$_2$] was isolated in 96% yield by metalation of {Carb^{DiPP}}H with KH. Solvent coordination appears to be loose, and thf can be removed under dynamic vacuum. XRD analysis of the yellow [{Carb^{DiPP}}K.thf] (Fig. S22) revealed a distorted tetrahedral geometry around potassium, with K-N interatomic distances (2.6479(11)-2.7332(11) Å) within the known ranges for potassium-diiminocarbazolates.[38] The stoichiometric reaction of [{Carb^{DiPP}}K.(thf)$_2$] and BaI_2 in thf affords [{Carb^{DiPP}}BaI.(thf)$_2$] (**3**) as a yellow solid in near quantitative yield (see Scheme 1). The complex crystallises as a di-solvated monomer (Fig. 4). The six-coordinate metal centre rests in a distorted anti-prismatic geometry. The three Ba-N interatomic distances are fairly comparable, in the range 2.726(2)-2.801(2) Å, and commensurate with those in **1**. The Ba-I bond length, 3.4052(3) Å, matches that for reported barium iodides.[34,39-40]

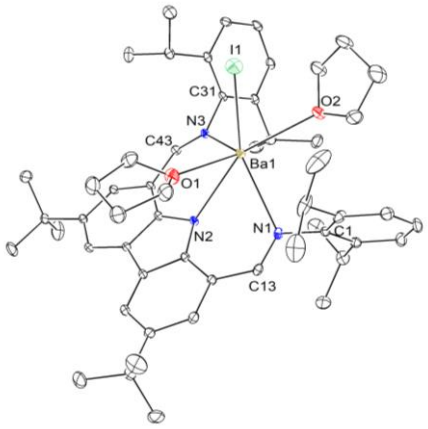

Figure 4. Displacement ellipsoids (30% probability; H atoms omitted) for [{Carb^{DiPP}}BaI.(thf)$_2$] (**3**). Representative interatomic distances (Å) and angles (°): Ba1-I1 = 3.4052(3), Ba1-N1 = 2.788(2), Ba1-N2 = 2.726(2), Ba1-N3 = 2.801(2), Ba1-O1 = 2.734(2), Ba1-O2 = 2.778(2); N2-Ba1-I1 = 141.39(4), N1-Ba1-N3 = 127.69(6).

Compounds **2** and **3** were then tested as synthetic precursors to obtain (yet unknown) heteroleptic barium-tetrelides. While the strong Ba-F bond (ΔH_f = 487(7) kJ mol^{-1}) in **2** proved reluctant to react with $NaNH_2$ or $Si(SiMe_3)_4$, **3** reacted cleanly in salt metathesis reactions. Hence, [{Carb^{DiPP}}BaSi(SiMe$_3$)$_3$.thf] (**4**), the first heteroleptic Ba-silanylide and only the second example of a Ba-silanylide,[32] was obtained by equimolar reaction of **3** with the bulky [KSi(SiMe$_3$)$_3$.(thf)$_2$].[41] Orange crystals suitable for XRD analysis were isolated in a 36% (non-optimised) yield. The monomeric **4** is soluble in common organic solvents, including aliphatic hydrocarbons. The ^{29}Si{^{1}H}-INEPT NMR spectrum of **4** displays two sharp resonances, a major one at δ_{29Si} = –5.8 ppm for Si(*Si*Me$_3$)$_3$, and a minor one, at –158.3 ppm, assigned to *Si*(SiMe$_3$)$_3$. The chemical shifts are consistent with those for the homoleptic [Ae(Si(SiMe$_3$)$_3$)$_2$.(thf)$_n$],[26,29] although no value was reported for the barium-bound Ba-*Si*(SiMe$_3$)$_3$ Si atom in this series. The molecular structure of **4** established by XRD analysis is depicted in Fig. 5. The crystallographically C_s-symmetrical molecule is disordered over several sites including, very typically, Si(SiMe$_3$).[42] The geometry around the five-coordinate Ba atom forms a distorted square pyramid (τ_5 = 0.25), with the Si(SiMe$_3$)$_3$ in apical position. This square pyramidal arrangement driven by the chelating nature of the carbazolate ligand is consistent with the hypervalent 12-electron count of Ba. The Ba-Si interatomic distance averaged over the two occupancy sites, 3.403(4)$_{av}$ Å, is close to those in [Ba(Si(SiMe$_3$)$_3$)$_2$.(thf)$_4$] (3.419(1) and 3.461(1) Å).[32] Significant pyramidalisation at the silicon atom Si1a, with compressed Si(i)-Si1a-Si(j) angles (i, j = 2a, 3a, 4a) in the range

101.68(14)-101.93(14)° and, by opposition, large Ba1-Si1a-Si(i) angles (107.01(12)-126.44(12)°) in **4**, indicate substantial metal-to-ligand charge transfer from Ba to Si1a.[43] As in **2**, the Ba-$N_{carbazolate}$ bond length in **4** (2.626(3) Å) is shorter than the Ba-N_{imine} ones (2.776(4) and 2.795(3) Å). All corresponding Ba-N bonds are shorter in the Ba-silanylide than in **2**, reflecting lower steric pressure and coordination number, and hence stronger bonds, in the former.

The Ba-iodide **3** also reacted with [$KSn(SiMe_3)_3.(thf)_n$] (prepared in situ[44]) to afford [{$Carb^{DiPP}$}$BaSn(SiMe_3)_3$.thf] (**5**), the

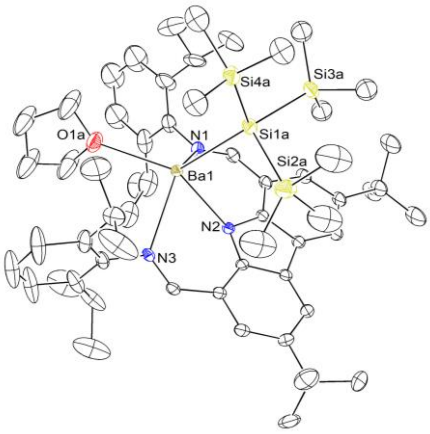

Figure 5. Displacement ellipsoids (30% probability; H atoms omitted) for [{$Carb^{DiPP}$}$BaSi(SiMe_3)_3$.thf] (**4**). Only the main components of the disordered thf, ^{t}Bu, ^{i}Pr and $Si(SiMe_3)_3$ shown. Selected interatomic distances (Å) and angles (°): Ba1-N1 = 2.776(4), Ba1-N2 = 2.626(3), Ba1-N3 = 2.795(3), Ba1-O1A = 2.729(4), Ba1-Si1A = 3.460(3), Ba1-Si1B = 3.346(4) (not shown), Si1A- Si2A = 2.362(3), Si1A-Si3A = 2.354(3), Si1A- Si4A = 2.358(3); Si2A-Si1A-Si3A = 101.93(14), Si2A-Si1A-Si4A = 101.68(14), Si3A-Si1A-Si4A = 101.79(14), Ba1-Si1A-Si2A = 107.01(12), Ba1-Si1A- Si3A = 114.82(12), Ba1-Si1A-Si4A = 126.44(12), N2-Ba1-Si1A = 98.12(9), N1-Ba1-N3 = 122.86(12). Site occupancy for $Si(SiMe_3)_3$: a, 57% ; b, 43%.

first barium stannylide with an unsupported Ba-to-Sn bond, as an orange solid upon removal of KI. Complex **5** is characterised by a sharp resonance at δ_{119Sn} = –758 ppm in its $^{119}Sn\{^1H\}$ NMR spectrum. The $^{29}Si\{^1H\}$-INEPT spectrum exhibits a sharp singlet at δ_{29Si} = –10.4 ppm, with clearly detectable ^{119}Sn and ^{117}Sn satellites ($^1J_{29Si\text{-}119Sn}$ = 83 Hz, $^1J_{29Si\text{-}117Sn}$ = 73 Hz). Both of these resonances are substantially shifted towards lower fields compared to the crown-ether adduct $[Li(12c4)]^+[(Me_3Si)_3Sn]^-$ (–882 and –12.9 ppm) or also to its heavier alkali congeners,[47] while the $^1J_{29Si\text{-}119Sn}$ and $^1J_{29Si\text{-}117Sn}$ coupling constants are much greater in this compound (204/195 Hz resp.) than in **5**. The Ba-stannylide **5** is isomorphous with its silanylide congener **4**. The arrangement about Ba1 forms a C_s-symmetrical distorted square pyramid (τ_5 = 0.28), with disorder over several positions (Fig. 6, with 58% occupation for the main $Sn(SiMe_3)_3$ site). The average Ba-Sn interatomic distances in **5** of $3.521(3)_{av}$ Å is longer than the corresponding Ba-Si one in **4** ($3.403(4)_{av}$ Å). This difference is lower than expected on the basis of the covalent radii for Si and Sn (1.20 and 1.39 Å), supposedly owing to the softer and more polarisable nature of tin. The pyramidalisation at *Sn*$(SiMe_3)_3$ in **5** is greater than for the silicon atom *Si*$(SiMe_3)_3$ in **4**. Hence, the Si(i)-Sn1a-Si(j) angles all fall within 97.06(18)-99.17(18)°, i.e. relatively close to the value of 90° expected for a three-coordinate tin(II) due to its lower ability for hybridisation between *s* and *p* orbitals. Conversely, the Ba1-Sn1a-Si(i) angles are large, between 107.63(14)-132.71(11)°. Based on these structural data, it is therefore tempting to consider an ionic model for **5**, with barium-to-tin electron transfer resulting in a barium cation and a negatively charged tin(II) anion. Compression of the Si(i)-Sn1a-Si(j) angles and pyramidalisation in **5** are greater than in the NHC-ligated [{:C{N(^{i}Pr)C(Me)}$_2$}Sn{$Sn(SiMe_3)_3$}$_2$] (Si-Sn-Si_{av} = 104.7(5)°) or in [Mg{$Sn(SiMe_3)_3$}$_2$.$(thf)_2$] (103.9(5)°),[45-46] but similar to those in the ionic salts [$LiSn(SiMe_3)_3.(thf)_3$] (98.8(2)°)[48] and [{15-c-5}$NaSn(SiMe_3)_3$] (99.1(3)°).[47] The $N_{carbazolate}$-Ba-Sn angle in **5** (94.46(12)°) is narrower than the corresponding $N_{carbazolate}$-Ba-Si angle in **4** (98.12(9)°) due to the release of steric congestion between $SiMe_3$ and backbone ^{t}Bu groups on switching from Si to the larger Sn.

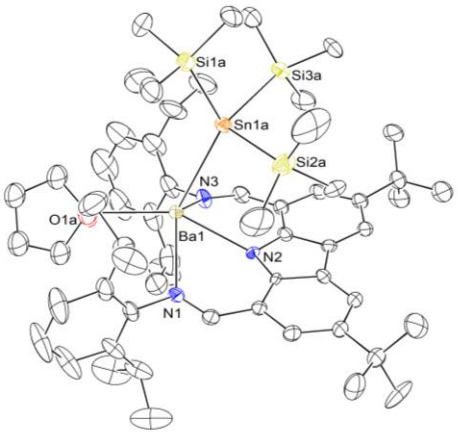

Figure 6. Displacement ellipsoids (30% probability; H atoms omitted) for [{$Carb^{DiPP}$}$BaSn(SiMe_3)_3$.thf] (**5**). Only the main components of the disordered thf, ^{t}Bu, ^{i}Pr and $Sn(SiMe_3)_3$ sites are shown. Representative interatomic distances (Å) and angles (°): Ba1-N1 = 2.752(5), Ba1-N2 = 2.637(5), Ba1-N3 = 2.728(6), Ba1-O1A = 2.711(14), Ba1-Sn1A = 3.5813(18), Ba1-Sn1B = 3.461(3) (not shown), Sn1A-Si1A = 2.572(4), Sn1A-Si2A = 2.575(5), Sn1A-Si3A = 2.580(5); Si1A-Sn1A-Si2A = 99.17(18), Si1A-Sn1A-Si3A = 97.06(18), Si2A-Sn1A-Si3A = 97.57(17), Ba1-Sn1A-Si1A = 132.71(11), Ba1-Sn1A-Si2A = 107.63(14), Ba1-Sn1A-Si3A = 116.51(13), N2-Ba1-Sn1A = 94.46(12), N1-Ba1-N3 = 126.43(19). Site occupancy for $Sn(SiMe_3)_3$: a, 58% ; b, 42%.

Table 1. Representative structural features for complexes **1**-**5** (R = $SiMe_3$).

Barium complex		Nucl.[a]	C.N.[b]	THF/ Ba	N_i^N_{carb}^N'_i angle[c]	N_i^Ba^N'_i angle[d]	Ba distance to plane[e]
Ba-NR_2	(**1**)	1	4	0	106.9(1)	133.1(1)	0.824
Ba-F	(**2**)	2	7	1.5	103.9(1)	112.9(1)	1.657
Ba-I	(**3**)	1	6	2	106.0(1)	127.7(1)	1.172
Ba-SiR_3	(**4**)	1	5	1	103.7(1)	122.9(1)	1.349
Ba-SnR_3	(**5**)	1	5	1	104.4(2)	126.4(2)	1.187

[a] Nuclearity. [b] Coordination number. [c] N_{imine}-$N_{carbazolate}$-N'_{imine} angle (°). [d] N_{imine}-Ba-N'_{imine} angle (°). [e] Distance (Å) to the best $N(C)_3N(C)_3N$ backbone plane.

Examination of the coordination spheres in **1**-**5** reveals that the carbazolate ligand {Carb^{DiPP}}$^-$ gives access to a range of new barium complexes with a diversity of structural patterns; the main features are collated in Table 1. In particular, the data for mononuclear complexes **1** and **3**-**5** show that the ligand readily accommodates coordination numbers from 4 to 7, and is flexible enough to widen the N_{imine}-$N_{carbazolate}$-N'_{imine} angle up to at least 106.9(1)°, that is, almost 10° more than in the proligand {Carb^{DiPP}}H. The increase of this angle is paired with that of the N_{imine}-Ba-N'_{imine} angle and, concomitantly, a decrease of the distance from Ba to the best $N(C)_3N(C)_3N$ plane.

The bonding features in the Ba-tetrelide complexes **4** and **5** were probed by DFT calculations at the PBE0/TZP/Zora/D3 level (see SI). Their DFT-optimised geometries reproduce nicely the corresponding X-ray structures. The computed Ba-Si/Sn distances (3.279 and 3.438 Å, respectively) are somewhat shorter than their average X-ray counterparts, yet close to that found for the sites of minor statistical occupation (Fig. 5 and 6). These results suggest that the DFT Ba-Si/Sn distances in **4** and **5** are likely to be more reliable than their averaged counterparts from the disordered X-ray structures. Also, the computed ^{1}H and ^{13}C NMR chemical shifts are in an excellent agreement with their experimental counterparts (Fig. S31-S34). As expected, both **4** and **5** exhibit a substantial HOMO-LUMO gap (2.77 and 2.67 eV, respectively), which is however smaller than in the non-tetrelide complexes **1**-**3** (3.65, 3.75 and 3.74 eV, respectively). This is due to the higher energy of the HOMOs of **4** and **5**, which can be identified as their σ(Ba-Si/Sn) bonding orbital (Fig. 7). HOMOs of similar nature were found in related Ca-Sn species.[23] This HOMO is largely polarised on the tetrelide atom (84% and 73%, for Si/Sn *vs.* 5% and 12% on Ba for **4** and **5**, respectively). In any case, it is sufficiently bonding to confer some covalent character to the Ba-tetrel bond, as exemplified by the non-negligible Wiberg indices of 0.155 and 0.192 in **4** and **5**, respectively. These values are larger than that of the Ba-N(SiMe$_3$)$_2$ bond in **1** (0.09), but comparable to that of the Ba-I bond in **3** (0.150). It is also supported by the Ba natural atomic orbital (NAO) charge (1.76 and 1.74 in **4** and **5**, respectively), which is lower than in the more ionic complexes **1** and **2** (1.81 and 1.83, respectively) but closer to that in **3** (1.77). To further investigate the nature of the Ba-tetrelide interaction, a Morokuma-Ziegler energy decomposition analysis[49] was carried out, considering the interaction between the [Si/Sn(SiMe$_3$)$_3$]$^-$ and [{Carb^{DiPP}}Ba(thf)]$^+$ fragments in **4** and **5**. Assuming this heterolytic cleavage, the contribution of the orbital interaction to the total bonding energy amounts to 30% of that of the electrostatic component in both **4** and **5** (Table S30). This value, comparable to that for the Ba-I derivative in **3** (28%), is also indicative of weak but non-negligible covalent bonding. This (partly) covalent character of the Ba-to-tetrel bond can be attributed to the softer (less electronegative) nature of Si, Sn and I, as compared to the harder O- or N-ligands. The ionocovalent character of the donor-acceptor tetrel-Ba bond is further supported by a Quantum Theory of Atoms in Molecules (QTAIM)[50] analysis of **4** and **5**, where bond paths and bond critical points (BCPs) are found for the Ba-tetrel contacts. These BCPs are associated with weak electron densities (resp. 0.026 and 0.024 a.u.), small positive Laplacian values (resp. 0.030 and 0.027 a.u.), as well as small negative local energy density (resp. –0.004 and –0.003 a.u). Finally, the computed ^{119}Sn NMR chemical shifts for **5** (δ_{119Sn} = –993 ppm) and a selection of more covalent Sn-containing compounds (–112/–127 ppm) taken from the literature[51-54] correlate well with their experimental data (Fig. S35) and reflect the prevailing ionic character of the Ba-to-Sn bond in **5**. A similar reasoning can be drawn for the Ba-Si bond in **4** (Fig. S36).

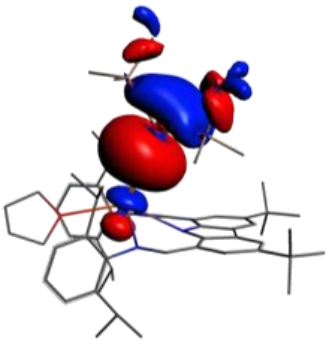

Figure 7. Plot of the HOMO of [{Carb^{DiPP}}BaSn(SiMe$_3$)$_3$.thf] (**5**; isovalue = 0.025 a.u.). That of the Ba-silanide complex **4** looks very similar (see Fig. S37).

Conclusion

In conclusion, the carbazole-based proligand {Carb^{DiPP}}H hence constitutes a most convenient entry point in the synthetic molecular chemistry of barium. Like the popular β-diketimine {BDI^{DiPP}}H that has proved so successful with calcium, it can be readily synthesised on large scales (up to 25 g, not optimised) in a few days. Yet, {Carb^{DiPP}}H alone enables the preparation of a variety barium species that are stable for weeks even at elevated temperature; this cannot be achieved with the regular {BDI^{DiPP}}$^-$ ligand. Along with the syntheses of starting materials like the solvent-free Ba-amide **1** (also a very effective precatalyst for styrene hydrophosphination that improves on state-of-the-art systems) and the Ba-iodide **3**, this has been illustrated upon successful productions of the first molecular Ba-fluoride **2**, and of **5**, the first compound with an unsupported Ba-to-Sn bond. DFT analysis of this Ba-stannylide **5** and its congeneric Ba-silanylide **4** indicates that the Ba-tetrelide bonds are chiefly ionic, although they feature a non-negligible covalent component. The versatility of {Carb^{DiPP}}H can be exploited to generate other heteroleptic species (e.g. alkyls, phosphides, hydrides) based on barium, but also calcium and strontium, as will be detailed in a forthcoming report. It thus opens up many opportunities for the further implementation of heavy alkaline earths in molecular catalysis and reactivity towards small molecules.

Acknowledgements

P.M.C, J.-F.C. and Y.S. thank the *Agence Nationale de la Recherche* for the provision of a research grant (ANR-17-CE07-0017-01). The GENCI (*Grand Equipment National de Calcul Intensif*) is acknowledged for HPC resources (Project A0050807367).

Keywords: barium • carbazolate • silanylide • stannylide • fluoride

[1] S. Harder, *Chem. Rev.* **2010**, *110*, 3852.

[2] M. R. Crimmin, M. S. Hill, *Top. Organomet. Chem.* **2013**, *45*, 191.
[3] M. S. Hill, D. J. Liptrot, C. Weetman, *Chem. Soc. Rev.* **2016**, *45*, 972.
[4] Y. Sarazin, J.-F. Carpentier, *Chem. Rec.* **2016**, *16*, 2482.
[5] M. Westerhausen, A. Koch, H. Görls, S. Krieck, *Chem. Eur. J.* **2017**, *23*, 1456.
[6] D. Mukherjee, D. Schuhknecht, J. Okuda, *Angew. Chem. Int. Ed.* **2018**, *57*, 9590.
[7] M. R. Crimmin, I. J. Casely, M. S. Hill, *J. Am. Chem. Soc.* **2005**, *127*, 2042.
[8] A. G. M. Barrett, C. Brinkmann, M. R. Crimmin, M. S. Hill, P. Hunt, P. A. Procopiou, *J. Am. Chem. Soc.* **2009**, *131*, 12906.
[9] P. Jochmann, J. P. Davin, T. P. Spaniol, L. Maron, J. Okuda, *Angew. Chem. Int. Ed.* **2012**, *51*, 4452.
[10] H. Bauer, M. Alonso, C. Färber, H. Elsen, J. Pahl, A. Causero, G. Ballmann, F. de Proft, S. Harder, *Nat. Catal.* **2018**, *1*, 40.
[11] H. Bauer, M. Alonso, C. Fischer, B. Rösch, H. Elsen, S. Harder, *Angew. Chem. Int. Ed.* **2018**, *57*, 15177.
[12] C. Bellini, J.-F. Carpentier, S. Tobisch, Y. Sarazin, *Angew. Chem. Int. Ed.* **2015**, *54*, 7679.
[13] D. J. Liptrot, M. S. Hill, M. F. Mahon, A. S. S. Wilson, *Angew. Chem. Int. Ed.* **2015**, *54*, 13362.
[14] A. G. Avent, M. R. Crimmin, M. S. Hill, P. B. Hitchcock, *Dalton Trans.* **2005**, 278.
[15] T. X. Gentner, B. Rösch, K. Thum, J. Langer, G. Ballmann, J. Pahl, W. A. Donaubauer, F. Hampel, S. Harder, *Organometallics* **2019**, 38, 2485.
[16] G. Ballmann, B. Rösch, S. Harder, *Eur. J. Inorg. Chem.* **2019**, 3683.
[17] X. Shi, C. Hou, C. Zhou, Y. Song, J. Cheng, *Angew. Chem. Int. Ed.* **2017**, *56*, 16650.
[18] B. Liu, T. Roisnel, J.-F. Carpentier, Y. Sarazin, *Angew. Chem. Int. Ed.* **2012**, *51*, 4943.
[19] X. Shi, G. Qin, Y. Wang, L. Zhao, Z. Liu, J. Cheng, *Angew. Chem. Int. Ed.* **2019**, *58*, 4356.
[20] C. Ruspic, S. Nembenna, A. Hofmeister, J. Magull, S. Harder, H. W. Roesky, *J. Am. Chem. Soc.* **2006**, *128*, 15000.
[21] C. Ruspic, S. Harder, *Inorg. Chem.* **2007**, *46*, 10426.
[22] S. Nembenna, H. W. Roesky, S. Nagendran, A. Hofmeister, J. Magull, P.-J. Wilbrandt, M. Hahn, *Angew. Chem. Int. Ed.* **2007**, *46*, 2512.
[23] L. J. Morris, M. S. Hill, I. Manners, C. L. McMullin, M. F. Mahon, N. A. Rajabia, *Chem. Commun.* **2019**, *55*, 12964.
[24] S. Sarish, S. Nembenna, S. Nagendran, H. W. Roesky, A. Pal, R. Herbst-Irmer, A. Ringe, J. Magull, *Inorg. Chem.* **2008**, *47*, 5971.
[25] S. Pillai Sarish, H. W. Roesky, M. John, A. Ringe, J. Magull, *Chem. Commun.* **2009**, 2390.
[26] M. Westerhausen, *Angew. Chem., Int. Ed. Engl.* **1994**, *33*, 1493.
[27] U. Englich, K. Ruhlandt-Senge, F. Uhlig, *J. Organomet. Chem.* **2000**, *613*, 139.
[28] W. Teng, K. Ruhlandt-Senge, *Organometallics* **2004**, *23*, 952.
[29] W. Teng, K. Ruhlandt-Senge, *Organometallics* **2004**, *23*, 2694.
[30] V. Leich, T. P. Spaniol, L. Maron, J. Okuda, *Angew. Chem. Int. Ed.* **2016**, *55*, 4794.
[31] D. Mukherjee, T. Höllerhage, V. Leich, T. P. Spaniol, U. Englert, L. Maron, J. Okuda, *J. Am. Chem. Soc.* **2018**, *140*, 3403.
[32] W. Teng, U. Englich, K. Ruhlandt-Senge, *Angew. Chem. Int. Ed.* **2003**, *42*, 3661.
[33] S. J. Malthus, S. A. Cameron, S. Brooker, *Inorg. Chem.* **2018**, *57*, 2480.
[34] J. Jenter, R. Köppe, P. W. Roesky, *Organometallics* **2011**, *30*, 1404.
[35] I. V. Lapshin, O. S. Yurova, I. V. Basalov, V. Y. Rad'kov, E. I. Musina, A. V. Cherkasov, G. K. Fukin, A. A. Karasik, A. A. Trifonov, *Inorg. Chem.* **2018**, *57*, 2942.
[36] E. Coz, H. Roueindeji, T. Roisnel, V. Dorcet, J-F. Carpentier, Y. Sarazin, *Dalton Trans.* **2019**, *48*, 9173.
[37] A. G. M. Barrett, M. R. Crimmin, M. S. Hill, P. B. Hitchcock, P. A. Procopiou, *Angew. Chem. Int. Ed.* **2007**, *46*, 6339.
[38] R. Nolla-Saltiel, A. M. Greer, W. Lewis, A. J. Blake, D. L. Kays, *Chem. Comm.* **2018**, *54*, 1825.
[39] A. Koch, S. Krieck, H. Görls, M. Westerhausen, *Organometallics* **2017**, *36*, 994.
[40] M. H. Chisholm, J. C. Gallucci, G. Yaman, *Dalton Trans.* **2009**, 368.
[41] C. Kayser, R. Fischer, J. Baumgartner, C. Marschner, *Organometallics* **2002**, *21*, 1023.
[42] C. Marschner, *Organometallics* **2006**, *25*, 2110.
[43] K. W. Klinkhammer, *Chem. Eur. J.* **1997**, *3*, 1418.
[44] J. Radebner, A. Eibel, M. Leypold, N. Jungwirth, T. Pickl, A. Torvisco, R. Fischer, U. K. Fischer, N. Moszner, G. Gescheidt, H. Stueger, M. Haas, *Chem. Eur. J.* **2018**, *24*, 8281.
[45] N. Katir, D. Matioszek, S. Ladeira, J. Escudé, A. Castel, *Angew. Chem. Int. Ed.* **2011**, *50*, 5352.
[46] D. Matioszek, N. Katir, S. Ladeira, A. Castel, *Organometallics* **2011**, *30*, 2230.
[47] R. Fischer, J. Baumgartner, C. Marschner, F. Uhlig, *Inorg. Chim. Acta* **2005**, *358*, 3174.
[48] C. J. Cardin, D. J. Cardin, W. Clegg, S. J. Coles, S. P. Constantine, J. R. Rowe, S. J. Teat, *J. Organomet. Chem.* **1999**, *573*, 96.
[49] F. M. Bickelhaupt, E. J. Baerends, *Rev. Comput. Chem.* in K. B. Lipkowitz D. B. Boyd, Eds.; Wiley, New York **2000**, *15*, 1.
[50] R. F. W. Bader, R. F. W. Atoms in Molecules-A Quantum Theory; Oxford University Press; Oxford, England, **1990**.
[51] H. Preut, H.-J. Haupt, F. Huber, *Z. Anorg. Allg. Chem.* **1973**, *396*, 81.
[52] M. Prager, U. Zachwieja, C. J. Carlile, *Physica B,* **1994**, *202*, 360.
[53] J. Baumgartner, R. Fischer, J. Fischer, A. Wallner, C. Marschner, U. Florke, *Organometallics* **2005**, *24*, 6450.
[54] J. Plotzitzka, C. Kleeberg, *Inorg. Chem.* **2016**, *55*, 4813.

Entry for the Table of Contents

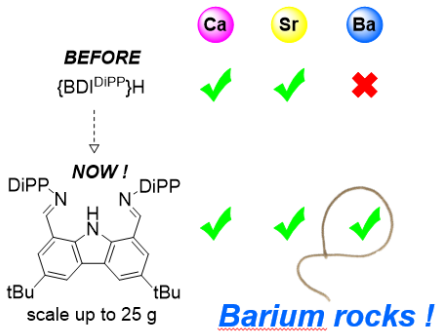

Ba fluoride, silanylide, stannylide !!!

A new carbazole-based ligand, readily available on large scales, enables the syntheses of yet unknown solution stable barium complexes, e.g. Ba-fluoride and Ba-stannylide species, that display unusual bonding patterns.